Triple-Quantum Two-Dimensional ^{27}Al Magic Angle Nuclear Magnetic Resonance Study of the Aluminum Incorporation in Calcium Silicate Hydrates

P. Faucon,*,† T. Charpentier,‡ A. Nonat,§ and J. C. Petit†

Contribution from the Service de Chimie Moléculaire, CEA Saclay, 91191 Gif sur Yvette, France, Service de Physique de l'Etat Condensé, CEA Saclay, 91191 Gif sur Yvette, France, and Laboratoire de Recherche sur la Réactivité du Solide, UMR 5613, CNRS−Université de Bourgogne, BP 400, 21011 Dijon, France

Received March 2, 1998. Revised Manuscript Received September 16, 1998

Abstract: Triple-quantum two-dimensional ^{27}Al magic angle spinning nuclear magnetic resonance (^{27}Al 3Q-MAS NMR) was used to characterize the substitution of Si^{4+} by Al^{3+} into the Te−Oc−Te structure of calcium silicate hydrates (C−S−H). This substitution was studied with C−S−H having an Oc/Te ratio of 1 and in equilibrium with $Al(OH)_3$ in aqueous suspensions. In the absence of NaOH, no substitution into the C−S−H structure occurred. Addition of NaOH in the preparation increased the concentration of $Al(OH)_4^-$ and favored substitution. The deficit of charge resulting from this substitution was compensated by the accommodation of sodium in the interlayer space of the C−S−H. Increasing levels of substituted silicon correspond to higher alkaline and lower calcium contents in the interlayer space. Two substitution sites were distinguished, corresponding to the bridging and nonbridging positions in the chains of tetrahedra. A high $Al_{tetra}/(Si+Al_{tetra})$ ratio indicated a redistribution of the aluminum tetrahedral sites to stabilize the substituted structure favoring aluminum in the bridging position.

Introduction

The structure of calcium silicate hydrates (C−S−H), poorly crystalline,[1] of variable composition (Ca/Si ranges between 0.66 to more than 1.5) may be subject to numerous substitutions. The investigation of such structures is therefore extremely difficult but magic angle spinning nuclear magnetic resonance (MAS NMR) has proven to be a valuable technique. For instance ^{29}Si MAS NMR has revealed the presence of silicate tetrahedra linear chains with variable length in the structure of the C−S−H.[3,4] At Ca/Si = 0.66, the ^{29}Si MAS NMR spectra of C−S−H and tobermorite are similar.[4] The resulting structure may be compared with the Te−Oc−Te smectite structure with tetrahedral sheets of SiO_2 linear chains (planes in the smectite) and a pseudooctahedral sheet of CaO polyhedra. The silicate tetrahedral chains are constituted of dimers connected by a bridging tetrahedron ("dreierketten" structure analogous to that of wollastonite).[5,6] Using the classical nomenclature, we will denote Si[Q2] those dimers connected by bridging tetrahedra and Si[Q2L] the bridging tetrahedra (Figure 1).

Each Si[Q2] shares all its oxygen with the calcium of the octahedral plane or with the Si[Q2L]. However, the Si[Q2L] tetrahedron has two unshared oxygen atoms which leaves a negative charge on the Te−Oc−Te unit. At Ca/Si = 0.66, H^+ ions situated in the "interlayer" space between the Te−Oc−Te unit provide the electrical neutrality. An increase of the Ca/Si ratio in the range 0.66−1 may be obtained by substituting these protons with calcium ions located in the interlayer space. Molecular dynamics simulations[7] have demonstrated that such a substitution makes the silicate tetrahedral chains unstable. The resulting rupture of the chains at increasing Ca/Si ratio can be detected by ^{29}Si MAS NMR,[4] which reveals the occurrence of Si[Q1] tetrahedra (chain-end tetrahedra) in the C−S−H structure. An increase of the Ca/Si ratio in the range of 1 to 1.5 is possible by both elimination of bridging tetrahedra and substitution of the protons with calcium ions in the interlayer space. This results in decreasing proportions of Si[Q2L] and Si[Q2] and in an increased population of Si[Q1] (as seen with ^{29}Si MAS NMR results).[8]

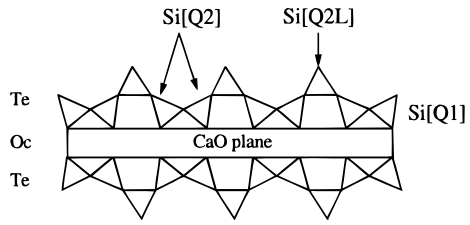

Figure 1. Silicate tetrahedra chains in the C−S−H.

By analogy with the smectite structure, numerous substitutions are expected in C−S−H. Previous works on ^{27}Al and/or ^{29}Si

† Service de Chimie Moléculaire.
‡ Service de Physique de l'Etat Condensé.
§ Laboratoire de Recherche sur la Réactivité du Solide.

(1) Xu, Z.; Viehland, D. *Phys. Rev. Lett.* **1996**, *77* [5], 952.
(2) Lippmaa, E.; Mägi, M.; Tarmak, M.; Wieker, W.; Grimmer, A. R. *Cem. Concr. Res.* **1982**, *12*, 597.
(3) Rodger, S. A.; Growes, G. W.; Clayden, N. J.; Dobson, C. M. *J. Am. Ceram. Soc.* **1988**, *71*, 91.
(4) Grutzeck, M.; Benesi, A.; Fanning, B. *J. Am. Ceram. Soc.* **1989**, *72*, 665.
(5) Hamid, S. A. *Z. Kristal.* **1981**, *154*, 189.
(6) Nonat, A.; Lecoq, X. in *NMR spectroscopy of Cement Based Materials*; Colombet, P., et al., Eds.; Springer-Verlag: Berlin, 1998; p 197.
(7) Faucon, P.; Delaye, J. M.; Virlet, J. *J. Solid State Chem.* **1996**, *127*, 92.
(8) Klur I. Thesis, 1996, Université Paris VI, France.

10.1021/ja9806940 CCC: $15.00
Published on Web 11/05/1998

MAS NMR[9−13] have demonstrated the substitution of silicon by aluminum in the tetrahedra chains. However, due to the broadening of spectral lines by the quadrupolar interaction, the discrimination between bridging and nonbridging tetrahedral aluminum sites could not be achieved by ^{27}Al MAS NMR. Likerwise, with ^{29}Si MAS NMR, the overlapping contributions of the various silicon sites (surrounded by aluminum or not) hampers definitive conclusions regarding the nature of the substituted sites.

Similar ambiguities exist with regard to the possible incorporation of Al^{3+} in the interlayer space.[11] Furthermore, Al^{3+} in octahedral sites of residual aluminum hydroxides in thermodynamic equilibrium with the C−S−H make the unambiguous detection by Al[27] MAS NMR of Al^{3+} in the interlayer space of the C−S−H difficult. In the octahedral sheet, calcium might also be substituted by aluminum, the charge excess being compensated by incorporation of the OH^- in the interlayer space as in the case of the AFm structure[14] or by the negative charge of the silicate tetrahedra. No evidence of the existence of this substitution has yet been presented in the literature.

These problems may be solved by using the multiple quantum magic angle spinning NMR experiment ("MQ-MAS"), which has been a valuable tool for better resolving the spectra of quadrupolar nuclei.[15] Continuing improvements to this new method[16−21] have allowed multisite crystalline components or glasses to be studied.[22−24] However, until now this technique has been rarely used on hydrate structures.[25,26] In a recent study,[26] the use of ^{27}Al 3Q-MAS NMR provided sufficiently resolved spectra to allow the detection of two tetrahedral aluminum sites in a C−S−H where silicon was substituted by aluminum. The purpose of this paper is thus to explore the different sites of silicon substitutions by aluminum as a function of the cations present in the interlayer space and the dependence of quadrupolar parameters, and isotropic chemical shifts of the substituted aluminum with respect to its second neighbors (H^+, Na^+, Ca^{2+}) are also reported.

MQ-MAS Theory

^{27}Al has 2I observable single quantum transitions, which can be separated into two groups: the central transition ($^1/_2 \leftrightarrow -^1/_2$) as well as others, often called satellite transitions. The central transition is not affected by the first-order quadrupolar interaction.[27] However, it suffers from a second-order quadrupolar broadening that is only partially averaged out by MAS. This interaction corresponds to the coupling between the quadrupolar moment of the nucleus and the electric field gradient originating from the local crystal field electronic environment (bonds, charges, ...). Two characteristic constants, the quadrupolar-coupling constant (C_Q) and the asymmetry parameter (η), are needed to describe it. C_Q and η are related to the quadrupolar frequency ν_Q by

$$\nu_Q = \frac{3C_Q}{2I(2I-1)}\sqrt{1+\frac{\eta^2}{3}} \qquad (1)$$

Apart from line broadening, the second-order quadrupolar interaction affects the position of the center of gravity of the central transition ($\delta_{1/2}$) which is shifted away from the position of the isotropic chemical shift.[28−30] For a $^5/_2$ spin like ^{27}Al the center of gravity of the central transition is given in ppm by:

$$\delta_{1/2} = \delta_{iso} - \frac{8}{30}\frac{\nu_Q^2}{\nu_o^2}10^6 \qquad (2)$$

where ν_o is its Larmor frequency and ν_Q its quadrupolar frequency. The whole sideband pattern of each external transition is also subjected to a shift $\delta_{(m,m-1)}$, similar to the expression of $\delta_{1/2}$ but with different numerical weighting factors for the quadrupolar contributions.

Several years ago, dynamic angle spinning (DAS) and double-rotation (DOR) methods were developed to increase the resolution of the NMR spectra of half-integer quadrupolar nuclei.[31−33] This was achieved by mutual annihilation of the broadening occurring in different complementary orientations of the rotation axis of the sample. However, both types of experiments require specially designed NMR probes and suffer limitations due to limited spinning rates (DOR) and due to dipolar evolution during the change of angle for abundant spins (DAS), which is the case for the aluminate hydrates.

Recently, a new method has been developed[15] that allows high-resolution spectra with a usual MAS probe to be obtained. In this method, called MQ-MAS, a coherence transfer within the multilevel system of the quadrupolar nuclei replaces the change of the spinning axis of the sample. This can be viewed as a coherence transfer echo or as a correlation of the evolution of a multiple-quantum (MQ) coherence ($m \leftrightarrow -m$; $m > {}^1/_2$) with that of the central one ($-^1/_2$, $^1/_2$). In the resulting two-dimensional (2D) spectrum, the projection of each 2D line shape on the two dimensions is used to determine the parameters of the site.[16,17] After a shearing transformation of the 2D spectrum,[34,35] the projection in the first dimension (the isotropic

(9) Richardson, I. G.; Brough, A. R.; Brydson, R.; Groves, G. W.; Dobson, C. M. *J. Am. Ceram. Soc.* **1993**, *76*, 2285.
(10) Richardson, I. G.; Brough, A. R.; Groves, G. W.; Dobson, C. M. *Cem. Concr. Res.* **1994**, *24*, 813.
(11) Kwan, S.; Larosa-Thompson, J.; Grutzeck, M. W. *J. Am. Ceram. Soc.* **1996**, *79*, 967.
(12) Faucon, P.; Adenot, F.; Jacquinot, J. F.; Virlet, J.; Jorda, M.; Cabrillac, R. *Proceedings of the 10th International Congress on the Chemistry of Cement*; Justnes, H., Ed.; Götborg, 1997; Vol. 3, 3v003.
(13) Richardson, I. G. *Proceedings of the 10th International Congress on the Chemistry of Cement*; Justnes, H., Ed.; Götborg, 1997; Vol. 2, 2ii068.
(14) Ahmed, S. J.; Taylor, H. F. W. *Nature* **1967**, *215*, 622.
(15) Frydman, L.; Harwood: J. S. *J. Am. Chem. Soc.* **1995**, *117*, 5367.
(16) Fernandez, C.; Amoureux, J. P. *Chem. Phys. Lett.* **1995**, *242*, 449.
(17) Massiot, D.; Touzo, B.; Trumeau, D.; Coutures, J. P.; Virlet, J.; Florian, P.; Grandinetti, P. J. *Solid State Nucl. Magn. Reson.* **1996**, *6*, 73.
(18) Massiot, D. *J. Magn. Reson. A* **1996**, *122*, 240.
(19) Amoureux, J. P.; Fernandez, C.; Steuernagel, S. *J. Magn. Reson. A* **1996**, *123*, 116.
(20) Wu, G.; Rovnyak, D.; Griffin, R. G. *J. Am. Chem. Soc.* **1996**, *118*, 9326.
(21) Kraus, H.; Prins, R.; Kentgens, A. P. M. *J. Phys. Chem.* **1996**, *100*, 16336.
(22) Baltisberger, J. H.; Xu, Z.; Stebbins, J. F.; Wang, S. H.; Pines, A. *J. Am. Chem. Soc.* **1996**, *118*, 7209.
(23) Feuerstein, M.; Hunger, M.; Engelhardt, G.; Amoureux, J. P. *Solid State Nucl. Magn. Reson.* **1996**, *7*, 95.
(24) Stebbins, J. F.; Xu, Z. *Nature* **1997**, *390*, 60.
(25) Hanaya, M.; Harris, R. K. *Solid State Nucl. Magn. Reson.* **1997**, *8*, 147.
(26) Faucon, P.; Charpentier, T.; Bertrandie, D.; Nonat, A.; Virlet, J.; Petit, J. C. *Inorg. Chem.* **1998**, *37*, 3726.
(27) Vega, A. J. In *The Encyclopedia of NMR*; Grant, D. M., Harris, R. K., Eds.; John Wiley and Sons: New York, 1995; p 3869.
(28) Frenzke, D.; Freude, D.; Frohlich, T.; Haase, J. *Chem. Phys. Lett.* **1984,** *111*, 171.
(29) Freude, D.; Haase, J.; Klinowski, J.; Carpenter, T. A.; Ronikier, G. *Chem. Phys. Lett.* **1985,** *119*, 365.
(30) Skibsted, J.; Nielsen, N. C.; Bildsoe, H.; Jakobsen, H. J. *J. Magn. Reson.* **1991**, *95*, 88.
(31) Llor, A.; Virlet, J. *Chem. Phys. Lett.* **1988**, *152*, 248.
(32) Samoson, A.; Lippmaa, E.; Pines, A. *Mol. Phys.* **1988**, *65*, 1013.
(33) Chmelka, B. F.; Mueller, K. T.; Pines, A.; Stebbins, J.; Wu, J.; Zwanziger, J. W. *Nature (London)* **1989**, *339*, 42.
(34) Grandinetti, P. J.; Baltisberger, J. H.; Llor, A.; Lee, Y. K.; Werner, U.; Eastman, M. A.; Pines, A. *J. Magn. Reson. A* **1993**, *103*, 72.

Table 1. Preparation of the C−S−H

	[NaOH][a] (mol/l)	Ca/(Si+Al)[a]	Al/Si[a]	Ca/(Si+Al)[b]	Al/Si[b]	Na/Si[b]	X results[b]
C−S−H(A0)	0	1.2	0	1.2	0	0	C−S−H
C−S−H(AI)	0	0.66	0.5	0.66	0.5	0	C−S−H + AH_3
C−S−H(AII)	0.5	0.66	0.5	0.59	0.5	0.2	C−S−H + AH_3
C−S−H(AIII)	1	0.66	0.33	0.75	0.33	0.35	C−S−H, AH_3, trace of residual ethanol used for the drying
C−S−H(AIV)	1	0.66	0.5	0.59	0.5	0.47	C−S−H, AH_3, trace of C_4AH_{13}
C−S−H(B)	−	−	−	1.1	0.32	−	C−S−H + C_2AH_8 + C_3AH_6

[a,b] Ratios given are molar ratios (*a*) of the initial preparation and (*b*) of the solid product after filtration; $AH_3 = Al(OH)_3$, $C_2AH_8 = [CaAl(OH)_4][OH(H_2O)_{1.5}]$, $C_3AH_6 = Ca_3Al_2(OH)_{12}$.

dimension) provides a spectrum without any broadening due to the second-order quadrupolar effect. For a $^5/_2$ spin such as that of ^{27}Al, the lines in that dimension of a 3Q-MAS NMR spectrum exhibit an "isotropic shift" δ_1:

$$\delta_1 = -\frac{17}{31}\delta_{iso} - \frac{8}{93}10^6\frac{\nu_Q^2}{\nu_o^2} \quad (3)$$

The expression is similar to that for ($\delta_{1/2}$), differing only in the numerical weighting factors for the chemical shielding and the quadrupolar contributions. If the coherence transfer is complete, a slice of the 2D 3Q-MAS spectrum at each site and corresponding position δ_1 gives in the second dimension (sometimes called the "MAS dimension") a line shape that is identical to the corresponding line in the MAS only spectrum. The position of the center of gravity of this "MAS" projection of the 3Q-MAS spectrum has exactly the same expression ($\delta_{1/2}$) as in the usual MAS spectrum. Thus, for ^{27}Al in a given resolved site, the measurement of the shifts δ_1 and $\delta_{1/2}$ of the two projections (isotropic and MAS) of the signal (central transition) allows easy separation and determination of the chemical shift δ_{iso} and the quadrupolar frequency ν_Q.

Due to the coherence transfer within the multilevel system of the quadrupolar nuclei, a MQ-MAS sequence will not be equally efficient for all the quadrupolar frequencies. This efficiency issue has been analyzed by several author;[36,37] the ^{27}Al 3Q MAS NMR sequence used in this paper was optimized to observe sites with a ν_Q value between 0.25 and 0.7 MHz.

Experimental Section

NMR Measurements. Solid-state ^{27}Al NMR spectra were acquired on a Brucker DMX-300 (7.1T) spectrometer operating at 78.617 MHz for ^{27}Al. A commercial MAS probe (4 mm) was used and the spinning speed was 12.5 kHz in all the experiments with an accuracy of ±5 Hz. For MAS experiments, the single pulse nutation angle was 15°. The 3Q-MAS spectra were acquired by using a combination of the Z-Filtering method[19] with rotor synchronization[18] and hypercomplex phase cycling[17] to obtain pure absorption spectra with greater sensitivity. With a radio frequency (rf) field strength of 140 kHz, the lengths of the first and second pulses were set to 2.5 and 0.8 μs, respectively. The third pulse was adjusted to be a selective 90° pulse on the central transition by using a rf field strength of 20 kHz and a pulse length of 4 μs. The delay (τ) between the second and the third pulse was set equal to two rotor periods (200 μs). The MAS and the 3Q-MAS spectra were accumulated with a recycle time of 1 s by using a high-power ^{1}H decoupling of 60 kHz. A home-built program especially optimized to perform the shear transformation was used to process the data.

The chemical shift and quadrupolar parameters were obtained, as explained above, in the following manner: the shift δ_1 was measured for each line from the projection of the 3Q-MAS spectrum in the isotropic dimension. Then, for each line at its δ_1 position, a slice was taken in the MAS dimension, with $\delta_{1/2}$ being the center of gravity of that MAS line shape. From these δ_1 and $\delta_{1/2}$ values, the isotropic chemical shift δ_{iso} and the quadrupolar frequency ν_Q were deduced from eqs 2 and 3. ^{27}Al isotropic chemical shifts (δ_{iso}) are reported in ppm relative to an external reference sample of 1.0 M $AlCl_3{\cdot}6H_2O$. The precision of the NMR parameters is on the last number of each given value.

^{29}Si MAS NMR spectra were recorded at the ^{29}Si frequency of 59.617 MHz, with a spinning speed of approximately 4 kHz in a double-bearing 7-mm ZrO_2 rotor. Spectra were accumulated by using single-pulse excitation and high-power ^{1}H decoupling with a 60 kHz rf field. A recycle time of 59 s was used. The number of scans was 800. $[Si(CH_3)_3]_8Si_8O_{20}$ was used as a secondary standard, with its major peak appearing at −11.6 ppm relative to tetramethylsilane (TMS, $Si(CH_3)_4$).

Samples. Series A of C−S−H was prepared from calcium hydroxide freshly decarbonated at 1000 °C for 24 h, silica (aerosil 200 Degussa), and gypsite (Extra pure Prolabo). C−S−H(A0) was synthesized without gypsite with use of a Ca/Si molar ratio of 1.2. All the other C−S−H of the series were prepared with the same initial Ca/(Si+Al) molar ratio (0.66) at different Al/Si ratios (Table 1). The raw materials were mixed with different NaOH concentrations in decarbonated water solution (water/solid = 50) (Table 1). The samples were stirred for 3 weeks at 25 °C and filtered. The C−S−H(A0) was stored at 100% humidity. The other samples were dried with acetone and then ether.

The C−S−H(B) (see Table 1) was a substituted C−S−H without sodium. Hydration of tricalcium silicate mixed with 15 wt % of tricalcium aluminate was made at a water/solid ratio of 0.38. The sample was kept in a lime saturated solution for 3 months and leached with demineralized water for a further 3 months at 25 °C. Successive samples were removed from the surface (in contact with the solution) to the core of the sample and lyophilized.[12] After carrying out a preliminary ^{27}Al MAS NMR study, we chose to perform the 3Q-MAS NMR spectrum on the sample that exhibited the strongest tetrahedral line.[12]

The chemical compositions of the solids and the mineralogical crystalline phases detected by X-ray diffraction are given in Table 1 (a cement nomenclature, where C = CaO, S = SiO_2, A = Al_2O_3, and H = H_2O, is employed throughout this paper).

Results

^{29}Si MAS NMR. The spectra of the different samples are given in Figure 2. The spectrum of C−S−H(A0) shows the characteristic lines of a nonsubstituted C−S−H. Recent dipolar correlations[8] on a similar sample have established the following assignments: Si[Q1] at −78 ppm, Si[Q2L] at −82 ppm, and Si[Q2] at −85 ppm. The Si[Q2L]/Si[Q2] ratio of about 0.5 in the spectrum confirms these assignments since, in the dreikette structure, one bridging tetrahedron is required to link two nonbridging tetrahedra.

The same three characteristic lines are found in the C−S−H(A1) spectrum. An overlapping of the Si[Q2L] and Si[Q2] lines is observed. The lower resolution on each line may be due to a higher dipolar broadening caused by the drying of the samples (AI to AIV). By contrast, the heteronuclear dipolar

(35) Grandinetti, P. J. In *Encyclopedia of Nuclear Magnetic Resonance*; Grant, D. M., Harris, R. K., Eds.; John Wiley and Sons: New York, 1995; p 1768.

(36) Medek, A.; Harwood, J. S.; Frydman, L. *J. Am. Chem. Soc.* **1995**, *117*, 12779.

(37) Amoureux, J. P.; Fernandez, C.; Frydman, L. *Chem. Phys. Lett.* **1996**, *259*, 347.

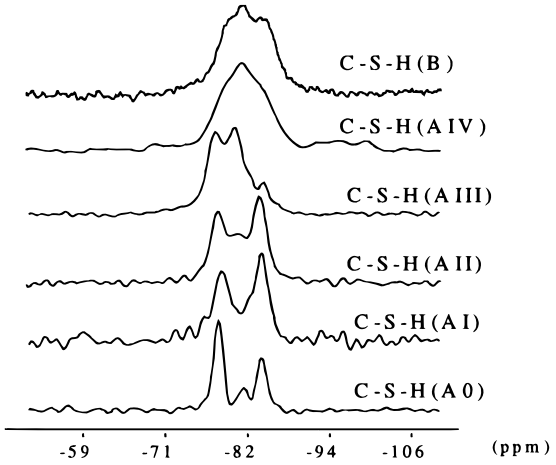

Figure 2. ^{29}Si MAS NMR spectra of the samples.

interaction between Si and H may be averaged, keeping the sample (A0) at 100% of humidity, due to the high mobility of the protons in the interlayer space in such conditions. The lower Si[Q1] contribution in this sample compared to that of the C−S−H(A0) sample demonstrates that the silicate chains are longer in the C−S−H(A1) sample**.** The spectrum does not allow us to conclude anything about the Si^{4+} substitution by Al^{3+} in the C−S−H structure.

In the C−S−H(AII) spectrum, a new line at about 81 ppm clearly appears. This line may be due to the substitution of silicon by aluminum in the silicate tetrahedra network, as can be confirmed by the ^{27}Al MAS NMR results. The presence of aluminum atoms as second neighbors in the tetrahedra network will decrease the Si chemical shift by about 4 ppm on the neighboring silicons.[38,39] The spectral lines of Si[Q2(1Al)] will therefore appear at about 81 ppm, Si[Q2L(1Al)] at −78.5 ppm, and Si[Q1(1Al)] at −74 ppm. The new line is thus a characteristic of Si[Q2(1Al)] and reveals the presence of aluminum in bridging positions, Al[Q2L], connected to the Si-[Q2] tetrahedra. The overlapping of the Si[Q2L(1Al)] and the Si[Q1] lines does not allow the possibility of some aluminum atoms in unbridging positions Al(Q2) to be distinguished. The same problem was found for all the samples investigated below.

In the C−S−H(AIII) spectrum, the line at −85 ppm attributed to the Si[Q2] has almost disappeared, which thus reveals a high degree of substitution of silicon by aluminum.

In the case of the C−S−H(AIV) and C−S−H(B) samples, the spectra are not sufficiently resolved and assigned to separate each line. However, comparison with the spectra of the C−S−H(A0, I,II,III) samples, and especially the line at −81 ppm, seems to validate the presence of aluminum in the chains.

For all the samples containing aluminum, ^{29}Si MAS NMR allows one to determine whether some silicon atoms have been substituted, but does not allow the position of the aluminum atoms in the tetrahedral chains to be distinguished. Similarly, no conclusions concerning the substitution of calcium by Al^{3+} in the octahedral plane or in the interlayer space can be made. The chemical shift of the ^{29}Si is not greatly affected by the presence of surrounding octahedral aluminum.

^{27}Al MAS NMR. Figure 3 presents the ^{27}Al MAS spectra for the samples. The spectrum of gypsite, $Al(OH)_3$, is also presented to identify its contribution to the spectra of the samples synthesized with it. Previous studies on aluminate hydrates by

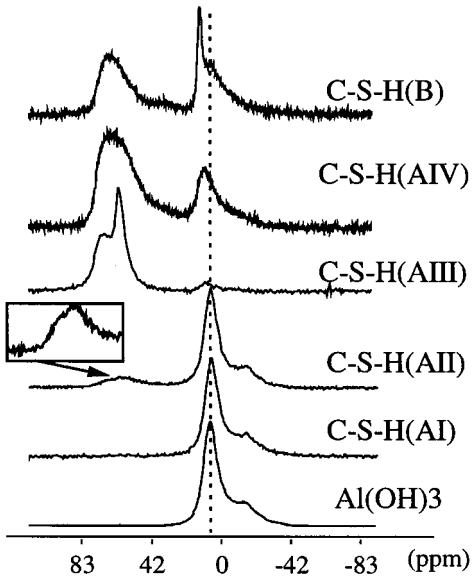

Figure 3. ^{27}Al MAS NMR spectra of the samples.

^{27}Al MAS[40,41] or ^{27}Al 3Q-MAS[26] NMR have given the characteristic NMR parameters of the two gypsite octahedral sites (Al(I): $\delta_{iso} = 11.9$ ppm and $\nu_Q = 0.67$ MHz, Al(II): $\delta_{iso} = 8.0$ ppm and $\nu_Q = 0.24$ MHz). The MAS spectrum is sufficiently resolved to detect these two sites.

The spectrum of C−S−H(AI) is clearly similar to the ^{27}Al MAS NMR spectrum of $Al(OH)_3$, a hydrate that is also detected by X-ray diffraction. In this C−S−H sample, the gypsite used to introduce aluminum is not fully dissolved and seems to be the only stable aluminum hydrate in these conditions.

Addition of NaOH in the synthesis (C−S−H(AII−AIV)) promotes the appearance of one or two lines at about 50 ppm, which can be attributed to tetrahedral aluminum. Such a value of chemical shift is often found for aluminum-substituting tetrahedral silicon.[39] This result is consistent with the ^{29}Si MAS NMR results and confirms the presence of tetrahedral aluminum in the silicate chains. With increasing NaOH concentration, most of the aluminum becomes tetrahedral. This is in agreement with the ^{29}Si MAS spectra which are characteristic of a high level of substitution of Si by Al.

In the C−S−H(AIII) sample, two tetrahedral lines are clearly identified. Taking into account that only C−S−H and gypsite are detected by X-ray diffraction in this sample (Table 1) and that amorphous hydrated silica does not appear on the ^{29}Si MAS NMR spectrum, the two tetrahedral sites can be attributed to the presence of aluminum in the C−S−H.

The spectrum of the C−S−H(AIV) sample is not sufficiently resolved to allow the identification of the expected tetrahedral contributions of aluminum. Two overlapping octahedral lines are clearly detected and the broad line can be attributed to one of the two sites present in gypsite. The second octahedral line does not correspond to the second gypsite line. Precipitation of a calcium aluminate may explain this new site, but the possibility of octahedral aluminum incorporation in the C−S−H must be taken into account as well.

In the case of the C−S−H(B) sample, prepared without sodium hydroxide, the octahedral contribution (at about 10 ppm) is sufficiently resolved on the ^{27}Al MAS spectrum to observe two lines. C_3AH_6 and C_2AH_8, detected by X-ray diffraction (Table 1), explain the presence of two octahedral sites in the

(38) Mägi, M.; Lipmaa, E.; Samoson, A.; Engelhardt, G.; Grimmer, A. R. *J. Phys. Chem.* **1984**, *88*, 1518.

(39) Engelhardt, G.; Michel, D. *High-Resolution Solid-State NMR of Silicates and Zeolites*; John Wiley and Sons: Chichester, 1987.

(40) Woessner, D. E. *Am. Mineral.* **1989**, *74*, 203.

(41) Skibsted, J.; Henderson, E.; Jakobsen, H. J. *Inorg. Chem.* **1993**, *32*, 1013.

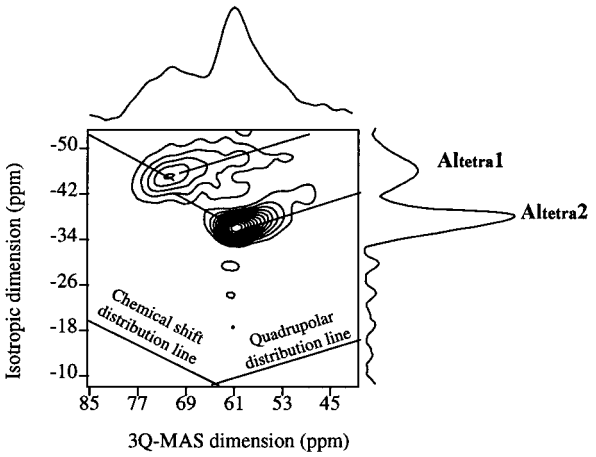

Figure 4. ^{27}Al 3Q-MAS NMR spectra of the C−S−H(AIII) sample with ^{1}H decoupling, in which the contour lines are drawn every 6.7%, starting at a level of 13.3% and ending at 93.3% of the maximum point in the spectrum. The spectrum is centered on the tetrahedral sites.

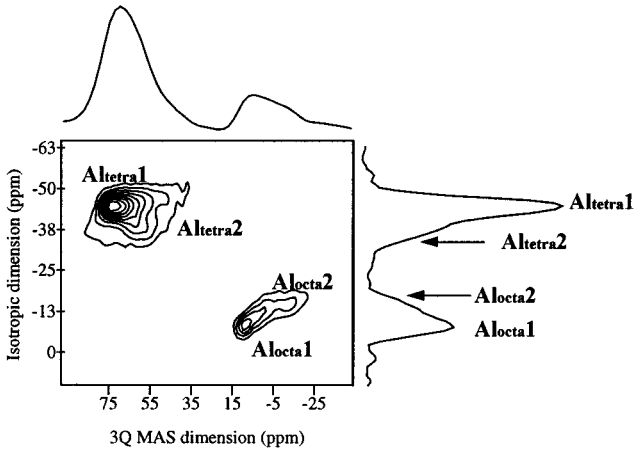

Figure 5. ^{27}Al 3Q-MAS NMR spectra of the C−S−H(AIV) sample with ^{1}H decoupling, in which the contour lines are drawn every 10%, starting at a level of 10% and ending at 90% of the maximum point in the spectrum.

Table 2. ^{27}Al NMR Parameters in the C−S−H (Accuracies: δ_{iso}, 0.5 ppm; ν_Q, 0.2 MHz)

site	δ_1 (ppm)	$\delta_{1/2}$ (ppm)	δ_{iso} (ppm)	ν_Q (MHz)	compound
$Al_{tetra}1$	−45.5	66.3	76.3	0.48	C−S−H(AIII), C−S−H(AIV)
$Al_{tetra}2$	−36.3	59.5	63.7	0.31	C−S−H(AIII), C−S−H(AIV)
$Al_{octa}1$	−8	5.5	11.2	0.35	C−S−H(AIV), C−S−H(B)
$Al_{tetra}1$	−42.6	63.4	72.5	0.45	C−S−H(B)

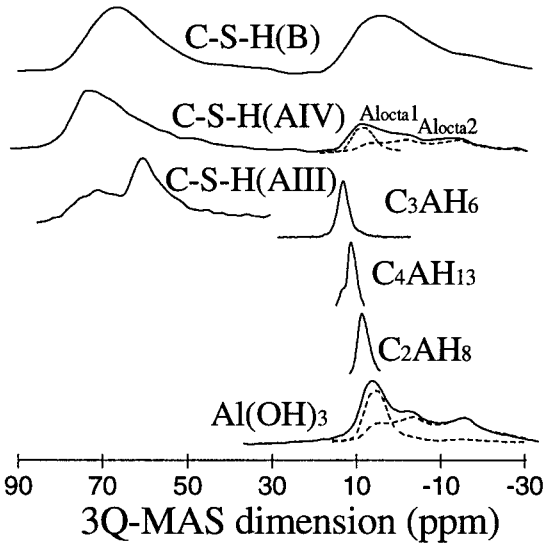

Figure 6. Projection in the 3Q MAS dimension of the ^{27}Al 3Q-MAS NMR spectra. Projections of C_3AH_6, C_2AH_8, C_4AH_{13}, and AH_3 are added following the results of Faucon et al.[26] ($C_4AH_{13} = [Ca_2Al(OH)_6](OH),3H_2O$).

sample. However, the broad line is not sufficiently resolved to reject the hypothesis of the presence of other sites, such as octahedral Al^{3+} in the C−S−H or in the amorphous aluminum hydroxide $Al(OH)_3$. The line at about 50−70 ppm is not sufficiently resolved to assign several tetrahedral sites.

For all samples, ^{27}Al MAS NMR allows an identification of the aluminum in the silicate chains of C−S−H that is in agreement with the ^{29}Si MAS NMR results. In the C−S−H(AIII) sample, two different tetrahedral aluminum sites were detected, but the parameters of the lines (δ_{iso}, ν_Q) cannot be obtained from the MAS spectrum. The assignment of the sites in the C−S−H structure is thus difficult. On the other hand, the occurrence of aluminum in the Ca plane or in the interlayer space of the C−S−H(AIV) and C−S−H(B) samples cannot be ruled out given the fact that the resolution of the octahedral lines is low. In these two cases, MQ-MAS was used to resolve these uncertainities.

^{27}Al 3Q MAS NMR of C−S−H(AI) and C−S−H(AII). The ^{27}Al 3Q-MAS spectra of the C−S−H(AI) and C−S−H(AII) samples are not given in this paper since they did not provide any information that was not already gained from the X-ray diffraction and the ^{27}Al MAS spectra.

^{27}Al 3Q MAS NMR of C−S−H(AIII). Figure 4 shows the ^{27}Al 3Q-MAS spectrum of the C−S−H(AIII) sample. The two tetrahedral contributions, already detected on the ^{27}Al MAS spectrum, are perfectly resolved. The good resolution allows a precise determination of the isotropic chemical shift and quadrupolar frequency for each line (i.e., $Al_{tetra}1$: $\delta_{iso} = 76.3$ ppm and $\nu_Q = 0.48$ MHz; $Al_{tetra}2$: $\delta_{iso} = 63.7$ ppm and $\nu_Q = 0.31$ MHz). As the 3Q-MAS projection (Figure 4) and the MAS spectrum (Figure 3) are approximately similar, the 3Q-MAS intensities of the two sites can be compared without recalibration by the coherence transfer efficiency. Using the isotropic projection of the 3Q-MAS spectrum, where the two tetrahedral contributions are perfectly resolved, we can calculate the actual distribution of aluminum in the C−S−H(AIII) sample: $Al_{tetra}1$, 30% and $Al_{tetra}2$, 70%.

^{27}Al 3Q MAS NMR of C−S−H(AIV). Figure 5 shows the ^{27}Al 3Q-MAS spectrum of the C−S−H(AIV) sample. Two overlapping tetrahedral sites are detected. The resolution is sufficient to conclude that the characteristics of each line, δ_1 and $\delta_{1/2}$, correspond to those of $Al_{tetra}1$ and $Al_{tetra}2$ in the C−S−H(AIII) sample (see Table 2). A higher content of $Al_{tetra}1$ sites, having a higher quadrupolar distribution (as observed in the C−S−H(AIII) sample), is responsible for the lower resolution of the tetrahedral contribution.

Two octahedral sites, $Al_{octa}1$ and $Al_{octa}2$, are observed in the 3Q-MAS spectrum (Figure 5). Figures 6 and 8 give respectively the MAS and the isotropic projections of the 3Q-MAS spectra for the C−S−H(AIV) sample and pure aluminate hydrates.[12] By using the MAS projections (Figure 6), $Al_{octa}1$ may be identified as a site of AH_3 or C_2AH_8 (not detected by X-ray diffraction). However, the isotropic projection of the $Al_{octa}1$ site is not consistent with this assignment (Figure 7): it does not correspond with the octahedral sites of the aluminate hydrates which may precipitate in the $CaO-Al_2O-H_2O$ system.[26] This is why $Al_{octa}1$, the approximate NMR parameters

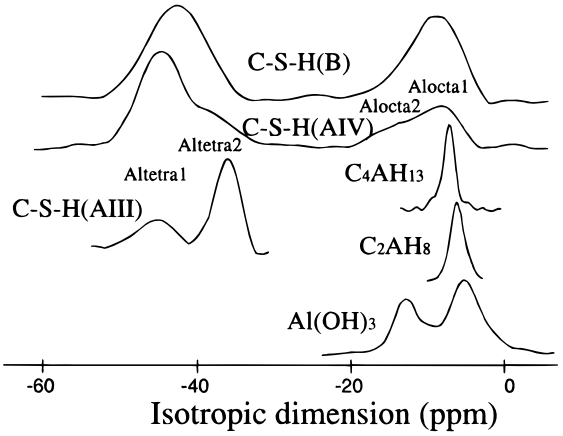

Figure 7. Projection in the isotropic dimension of the ^{27}Al 3Q-MAS NMR spectra. Projections of C_4AH_{13}, C_2AH_8, C_3AH_6, and $Al(OH)_3$ are added following the results of Faucon et al.[26]

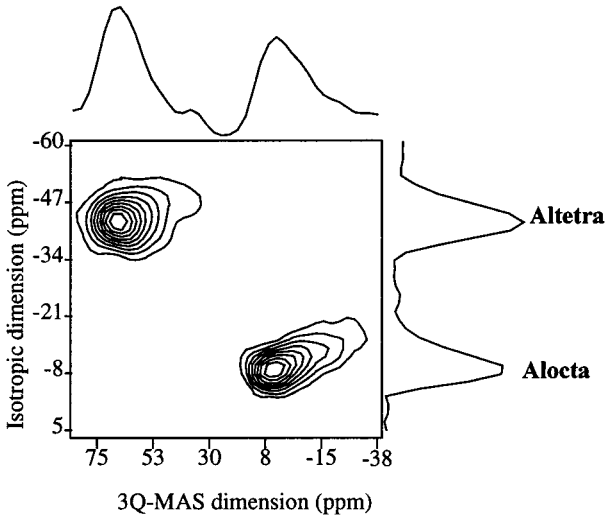

Figure 8. ^{27}Al 3Q-MAS NMR spectra of the C−S−H(B) with ^{1}H decoupling, in which the contour lines are drawn every 10%, starting at a level of 10% and ending at 90% of the maximum point in the spectrum.

of which are given in Table 2, might be octahedral aluminum in the C−S−H or in an AFm phase not detected by X-ray diffraction.

Figures 7 and 8 show that $Al_{octa}2$ is clearly the AH_3 site with the highest quadrupolar frequency (broad line). The second site of AH_3, with the smallest quadrupolar frequency (ν_Q = 0.24 MHz),[12] is not detected in the 3Q MAS experiments performed since its quadrupolar frequency corresponds to a low transfer efficiency.

^{27}Al 3Q MAS NMR of C−S−H(B). The ^{27}Al 3Q-MAS spectrum of the C−S−H(B) sample is given in Figure 8. A single tetrahedral site is detected with an isotropic chemical shift (72.5 ppm) lower than that of $Al_{tetra}1$ in the C−S−H of series A (76.3 ppm). Its quadrupolar frequency (0.46 MHz) is similar to the value found in series A for $Al_{tetra}1$.

The assignment of the octahedral contribution is quite difficult. Figures 6 and 8 show that the line may be characteristic of the aluminum site of C_2AH_8 (detected by X-ray diffraction) or of the AH_3 site (not detected by X-ray diffraction) with the highest quadrupolar frequency. The 3Q-MAS spectrum reveals a high quadrupolar distribution, which is characteristic of a high structural disorder. The $Al_{octa}1$ line, detected in the C−S−H(AIV) sample, may be detected in this sample. Due to a low quadrupolar frequency (ν_Q = 0.111 MHz) which results in a low transfer efficiency, C_3AH_6 is not detected in the 3Q-MAS experiment.

Mineralogy of the Samples. The stoechiometric ratios of the different samples may be deduced from both analytic and spectroscopic results. Quantification of aluminum in the different sites is possible because of the use of Π/12 pulses for all ^{27}Al MAS acquisitions.[42] Taking into account that all silicon and tetrahedral aluminum ions are in the C−S−H units (see ^{29}Si and ^{27}Al 3Q-MAS NMR results), the $Al_{tetra}/(Si+Al_{tetra})$ ratio of the C−S−H can be calculated for all the samples (Table 3).

In series A, the calcium content of the C−S−H is easily deduced by considering that all the calcium ions are in this compound. Knowing their calcium content, the $Ca/(Si+Al_{tetra})$ molar ratio of the C−S−H may be calculated (Table 3). The Na/Si ratio of the solids given in Table 1 is used to obtain the $Na/(Si+Al_{tetra})$ ratio in the C−S−H (Table 3). To better understand the structural changes possibly induced by substitutions in the C−S−H, it is useful to specify the Oc/Te molar ratio of the structure, which is the ratio between octahedral and tetrahedral sites. Octahedral sites are occupied by calcium and sodium and tetrahedral ones by aluminum and silicon. This ratio is then equal to $(Na+Ca)/(Si+Al_{tetra})$ and does not vary significantly from one sample to another (Table 3).

In the C−S−H(B) sample, the approximate calcium content cannot be deduced from the percentage of aluminum in the calcium aluminate hydrates because of the low resolution of the ^{27}Al MAS and 3Q MAS spectra. Thus in Table 3, only the $Al_{tetra}/(Al_{tetra}+Si)$ ratio is given.

Discussion

Substitution Sites. In all the samples, ^{29}Si MAS NMR spectra and ^{27}Al 3Q-MAS spectra demonstrate the incorporation of aluminum in the silicon tetrahedral network of C−S−H. Substitution of calcium in the octahedral sheet or incorporation of octahedral aluminum in the interlayer space may occur in the C−S−H(AVI) and C−SH(B) samples.

Referring to Table 2, three different aluminum sites may be distinguished in the tetrahedral environment of the C−S−H: $Al_{tetra}1$ and $Al_{tetra}2$ in series C−S−H(A) and Al_{tetra} in C−S−H(B). The ^{29}Si MAS NMR results show that these aluminum atoms substitute silicon atoms in Si[Q2] or Si[Q2L] tetrahedra. The isotropic chemical shift and quadrupolar parameters of Al_{tetra} are similar to the characteristics of the $Al_{tetra}1$, which has the highest isotropic chemical shift. By analogy with ^{29}Si MAS NMR results on the C−S−H(A0) sample where the highest chemical shift corresponds to the bridging tetrahedron (Si[Q2L] line, δ_{iso} = −82.5 ppm, − Si[Q2] line δ_{iso} = −85 ppm), it would be consistent to attribute the lines at δ_{iso} = 76.3 and 63.7 ppm detected in the C−S−H(A) sample to the Al[Q2L] and Al[Q2] sites, respectively, and the line at δ_{iso} = 72.5 ppm can be attributed to the Al[Q2L] site in the C−S−H(B) sample.

The quadrupolar frequencies of the sites confirm this assignment, and Ghose and Tsang[43] have shown a correlation of high quadrupolar frequencies with distortions of the Al coordinence polyhedron. Taking into account the higher distortion of the Q2L tetrahedra compared to the Q2 in the tobermorite structure,[5] Al[Q2L] will have a higher quadrupolar frequency than Al[Q2], as observed experimentally (Table 2).

The 3Q MAS spectra reveal that Al[Q2L] has a higher quadrupolar distribution than Al[Q2]. Al[Q2L] positions in the structure are more distributed than the Al[Q2] positions.

(42) Massiot, M.; Bessada, C.; Coutures, J. P.; Taulelle, F. *J. Magn. Reson.* **1992**, *90*, 231.

Table 3. Stoichiometry of the C−S−H Deduced from Analytical and NMR Results

	Al content (%)			C−S−H stoechiometry (molar ratio)			
	Al_{tetra} C−S−H	Al_{octa} AH_3	other Al_{octa} sites	$Ca/(Si+Al_{tetra})$	$Na/(Si+Al_{tetra})$	$Al_{tetra}/(Si+Al_{tetra})$	Oc/Te
C−S−H(AI)	−	100		0.99	0	0	0.99
C−S−H(AII)	16	84		0.82	0.19	0.07	1.01
C−S−H(AIII)	94	6		0.76	0.27	0.24	1.03
C−S−H(AIV)	68	<32	<32	0.66	0.35	0.26	1.01
C−S−H(B)	51	<39	<49	−	−	0.16	−

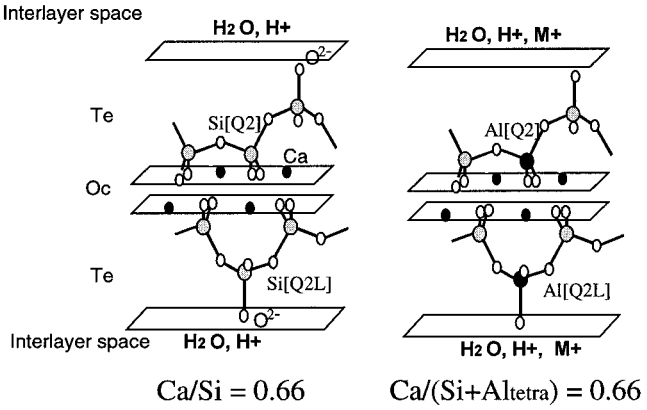

Figure 9. Substitution mechanism in the C−S−H: $[-\ Si_{tetra}-] + Al(OH)_4^-{}_{aq} + M^+{}_{aq} \rightarrow [-Al_{tetra}-]M_{interlayer} + H_4SiO_4$.

Charge Compensation. From the charge balance point of view, substitution of Si^{4+} by Al^{3+} in a MeO_4 tetrahedron results in a net negative charge. Referring to the Te−Oc−Te structure as a model for C−S−H, this negative charge may be compensated by monovalent cations in the interlayer space (Figure 9): H^+ in C−S−H(B) or Na^+ in the C−S−H(A) series. Calcium in the interlayer space promotes the disruption of the chain and is thus unfavorable for the substitution of Q2 or Q2L tetrahedra. The lower the calcium content of the structure (Table 3), the higher is the silicon substitution.

In the C−S−H(B) samples, aluminum in nonbridging sites was not detected. As the heterogeneity of this sample may be responsible for the lower resolution (see preparation method), we cannot conclude that Al[Q2] sites exist in such a sample with no alkalis. In the present C−S−H sample, they are clearly less favorable than the Al[Q2L] site. Interpretation of such a result would require the Ca/(Al+Si) ratio of the C−S−H (not calculated because of the broadening of the lines of the 3Q MAS spectrum). As previously discussed, a higher Ca/(Al+Si) ratio than in the C−S−H(A) series will change the C−S−H structure. This would modify the rules of Si^{4+} substitution by Al^{3+}. Further investigation is needed on C−S−H with high Ca/Si ratios.

Substitution Level. According to the Lowenstein rule, one might expect a maximum substitution level $Al_{tetra}/(Si+Al_{tetra}) = 0.5$ (Figure 10). This limiting value was never reached experimentally. The maximum value was about 0.26 for the C−S−H(AIV) sample, making the comparison with molecular dynamic calculations performed on the tobermorite structure with an $Al_{tetra}/(Si+Al_{tetra}) = 0.5$ ratio difficult.[44]

The reason for a maximum experimental $Al_{tetra}/(Si+Al_{octa})$ of 0.26 is probably the high electrostatic repulsion induced in the chains by the net negative charge carried by each aluminum-substituted site (Figure 10). A minimum distance between the substituted sites is required for stability. This is also probably

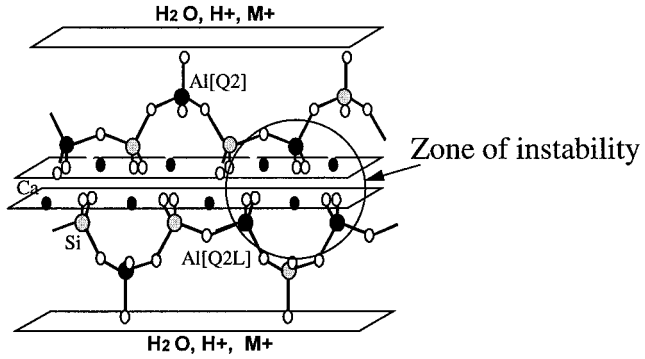

Figure 10. Theoretical level of maximum substitution in the C−S−H structure following the Lowstein rules.

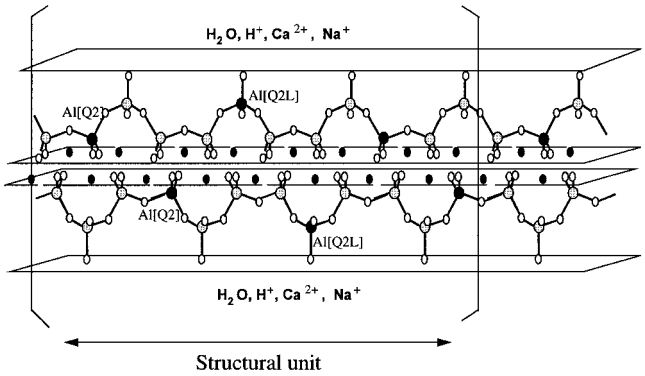

Figure 11. Shematic structure of the C−S−H in the C−S−H(AIII) sample: Altetra/(Si+Altetra) = 0.25, Al[Q2L]/Al[Q2] = Si[Q2L]/Si-[Q2] = 0.5.

the reason for the difference in the distribution between the Al-[Q2L] and Al[Q2] sites in the C−S−H(AIII) and C−S−H(AIV) samples.

In the C−S−H(AIII) sample the Al[Q2L]/A[lQ2] is about 0.4, not far from the Q2L/Q2 ratio of 0.5. Therefore, no preferential substitution of the Q2 or Q2L sites is expected in the C−S−H (Figure 11). In the C−S−H(AIV) sample, the substitution of one more silicon induces a repulsion of the Al neighbor to maintain at least two unsubstituted tetrahedra between them (Figure 12). The Al[Q2L] sites are thus preponderant, making the ^{29}Si MAS spectrum very different from the ^{29}Si MAS spectrum of the C−S−H(AIII) sample.

In the C−S−H(AIV) sample, the redistribution of the aluminum sites may lead to the incorporation of octahedral aluminum in the C−S−H structure (see ^{27}Al 3Q MAS results).

In series A, the increase of the NaOH concentration in solution makes it easier for the sodium and aluminum to be incorporated into the C−S−H structure. However, in the C−S−H(B) sample, a Al/(Si+Al) ratio of 0.14 is reached without addition of NaOH in solution. This demonstrates that substitution of Si^{4+} by Al^{3+} may be achieved without any alkali addition. The most important parameter is the concentration of $Al(OH)^{4-}$ species in solution: the calculated concentration

(43) Ghose, S.; Tsang, T. *Am. Mineral.* **1973**, *58*, 748.
(44) Faucon, P.; Jacquinot, J. F.; Delaye, J. M.; Virlet, J. *Philos. Mag. B* **1997**, *75*, No. 5, 769.

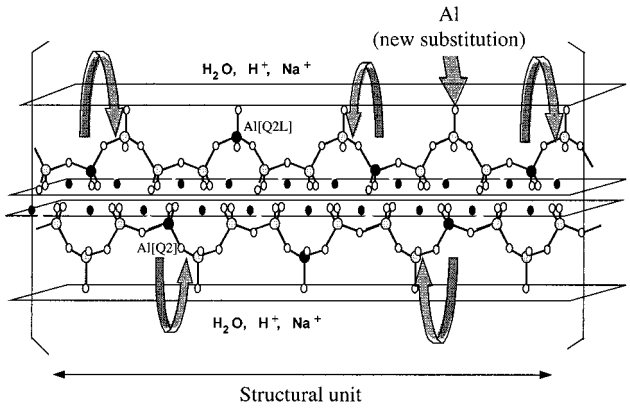

Figure 12. C−S−H structural evolution between the sample C−S−H(AIII) and C−S−H(AIV): $Al_{tetra}/(Si+Al_{tetra}) = 0.266$.

in the $CaO-SiO_2-Al_2O_3-H_2O$ system[46,47] is $[Al(OH)^{4-}] = 45$ mmol/L when C−S−H is equilibrated with C_2AH_8 and C_3AH_6 in water. In such a case, the experimental $Al_{tetra}/(Si+Al_{tetra})$ ratio found in the C−S−H(B) was 0.16. Similar calculations taking into account the dissolution of $Al(OH)_3$ in a 0.5 mol/L NaOH solution give $[Al(OH)^{4-}] = 15$ mmol/L. In the corresponding sample, C−S−H(AII), the $Al_{tetra}/(Si+Al_{tetra})$ ratio is 0.07. On the other hand, in the case of the C−S−H (AI) sample, synthesized without any addition of NaOH, the pH at equilibrium is relatively low (10.8) and $Al(OH)^{4-}$ does not exist in solution (only $Al^{3+}$is present at a concentration of 25 μmol/L). In these conditions, substitution of Si by Al is not observed. The pH augmentation due to the addition of NaOH increases the solubility of $Al(OH)_3$ and makes the $Al(OH)^{4-}$ species more stable. In a 1 mol/L NaOH solution, the $Al(OH)^{4-}$ concentration is enough to saturate the C−S−H in Al for the reasons explained above.

(45) Faucon, P.; Charpentier, T, P.; Henocq, P.; Petit, J. C.; Virlet, J.; Adenot, F. *Mater. Res. Soc.*; Proceedings of the Scientific Basis for Nuclear Waste Management XXI Symposium, Davos, 1997.

(46) Parkhurst, D. L., U.S. Geological Survey, Washington, 1980, USGS-WRI-80-96.

(47) Damidot, D.; Glasser, F. *Cem. Concr. Res*. **1995**, *25*, 22.

Conclusion

The ^{27}Al MAS-3Q NMR spectroscopy has been proven to be a powerful method for obtaining high-resolution NMR spectra in studies of silicon substitution by aluminum in calcium silicate hydrates (Oc/Te ratio = 1), where ^{29}Si and ^{27}Al MAS NMR gave little information. Coexisting with $Al(OH)_3$, no Si^{4+} substitution by Al^{3+} occurred in the C−S−H structure. Addition of NaOH in the preparation increased the $Al(OH)_4^-$ solubility and allowed the substitution. The deficit of charge resulting from substitution is compensated by sodium incorporated in the interlayer space of the C−S−H structure. Increasing levels of substituted silicon correspond to higher alkali content and lower calcium contents in the interlayer space. Two sites of silicon substituted by aluminum were identified, corresponding to the bridging and nonbridging positions in the chains of tetrahedra. High $Al_{tetra}/(Si+Al_{tetra})$ ratios require a redistribution of the aluminum tetrahedral sites to stabilize the substituted structure, making more favorable the bridging position for aluminum.

Due to the $Al(OH)_4^-$ concentration in the $CaO-SiO_2-Al_2O_3-H_2O$ system when C−S−H is equilibrated with C_2AH_8, silicon is also substituted by aluminum. Protons compensate the charge deficit resulting from this substitution. In the C−S−H investigated in this work, the substitution of the bridging tetrahedra (Q2L) seems then more favorable.

Further studies are needed to confirm the hypothesis of aluminum incorporation in the calcium octahedral sheet or (and) in the interlayer space of the C−S−H.

Acknowledgment. We express particular thanks to J. Virlet and M. Jacquinot, of the NMR laboratory of the CEA (Commissariat à l'Energie Atomique), for helpful discussions about the structure of the C−S−H. We express particular thanks to I. Lorgnot, and D. Bertrandie (Laboratoire de Réactivité des Solides, University of Bourgogne at Dijon, France) and F. Adenot (C.E.A) for the syntheses of the samples. We are also grateful to O. Araspin (C.E.A) for having studied our samples by scanning electron microscopy.

JA9806940